Extending Ground Motion Simulations to Higher Frequencies (f>1 Hz)

Robert Graves
U.S. Geological Survey

Talk Overview

- *Limitations of physics-based modeling*
- *Factors affecting low- and high-frequency strong ground motion*
- *Hybrid broadband simulations (low-frequency "deterministic" + high-frequency "stochastic")*

ShakeOut Scenario 2.0 Workshop
Oct. 6, 2026

USGS science for a changing world

Physics-Based EQ Ground Motion Simulations

- **Physics-based**–
  Result is determined by solving a set of physical conditions or equations (e.g., the wave equation)
- All physical models have some approximations
- More advanced physical models ***can*** yield more accurate representation of natural phenomena, but at the expense of mathematical complexity (***computation***) and expanded parameter space (***knowledge***).
- **Computational limitations**–
  Efficiency of algorithms, computer speed, storage capabilities, etc.
- **Knowledge limitations**–
  What we know and how well we know it

This is currently biggest hurdle

What controls strong ground motion?

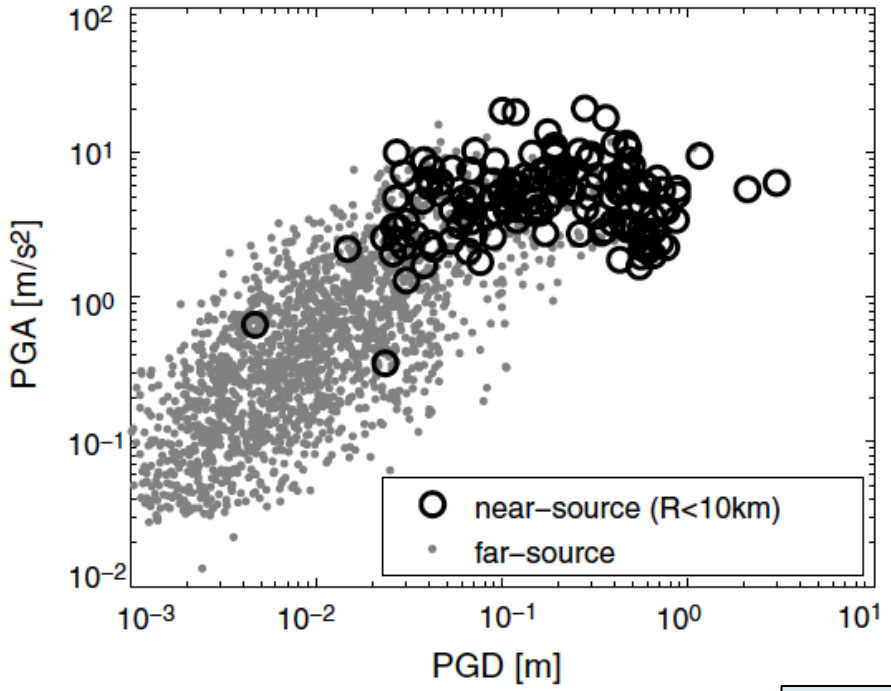

Yamada et al. (2009)

High frequency ground motions saturate near source;
Low frequency motions do not.

- Non-linear effects (source & site)
- Scattering and attenuation
- Large acceleration does not necessarily correlate with large slip, and in some cases, may negatively correlate

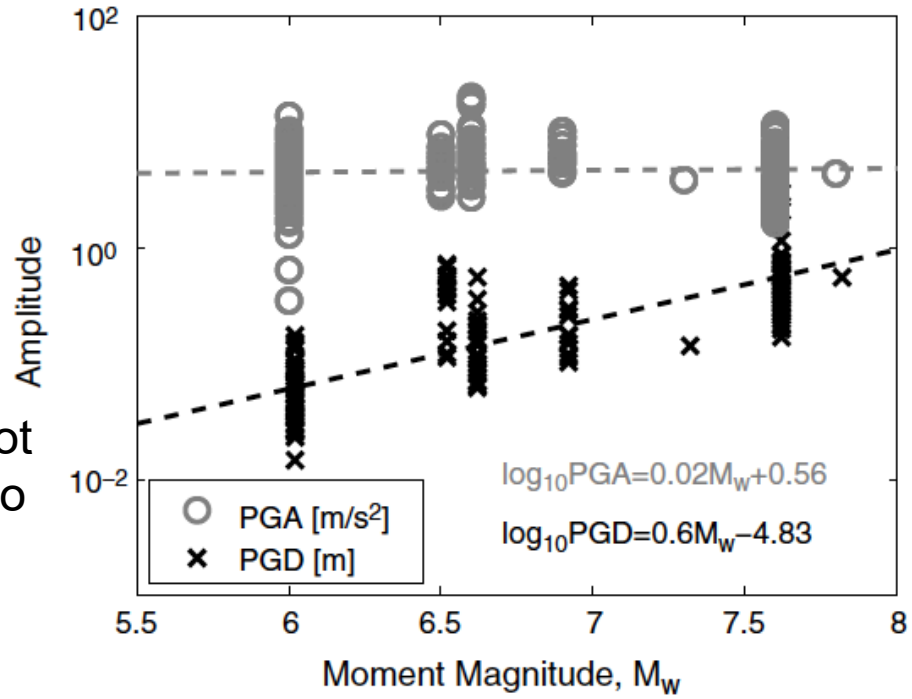

For **M**>6.5-7, median **PGA** does not increase; median **PGD** continues to increase with increasing **M**

What controls strong ground motion?

High Frequency (f > 1 Hz)

- Earthquake magnitude (**M**), distance from rupture (**R**) and site response
- For **M**>7, it is mainly **R** (magnitude saturation), site class being equal
- This is one reason why ground motion models (GMMs) work so well for higher frequencies

Low Frequency (f < 1 Hz)

- Magnitude (**M**), local fault slip (**D**), distance (**R**), hypocenter, radiation pattern, and large-scale geologic structure (basins, etc.)
- For example, being 5 km from a portion of the fault that slips 10 meters is quite different than being 5 km from a portion that slips 1/2 meter
- Large ruptures can have tremendous variability in slip along the fault, and hence a large variability in low frequency motions

Finite-Fault Rupture Effects

Rupture Directivity

- Primarily affects lower frequencies (f<1 Hz)
- **SH** motion sums coherently in direction of rupture propagation: ***Larger Fault Normal***
- **SV** motion is nodal in direction of rupture propagation: ***Smaller Fault Parallel***

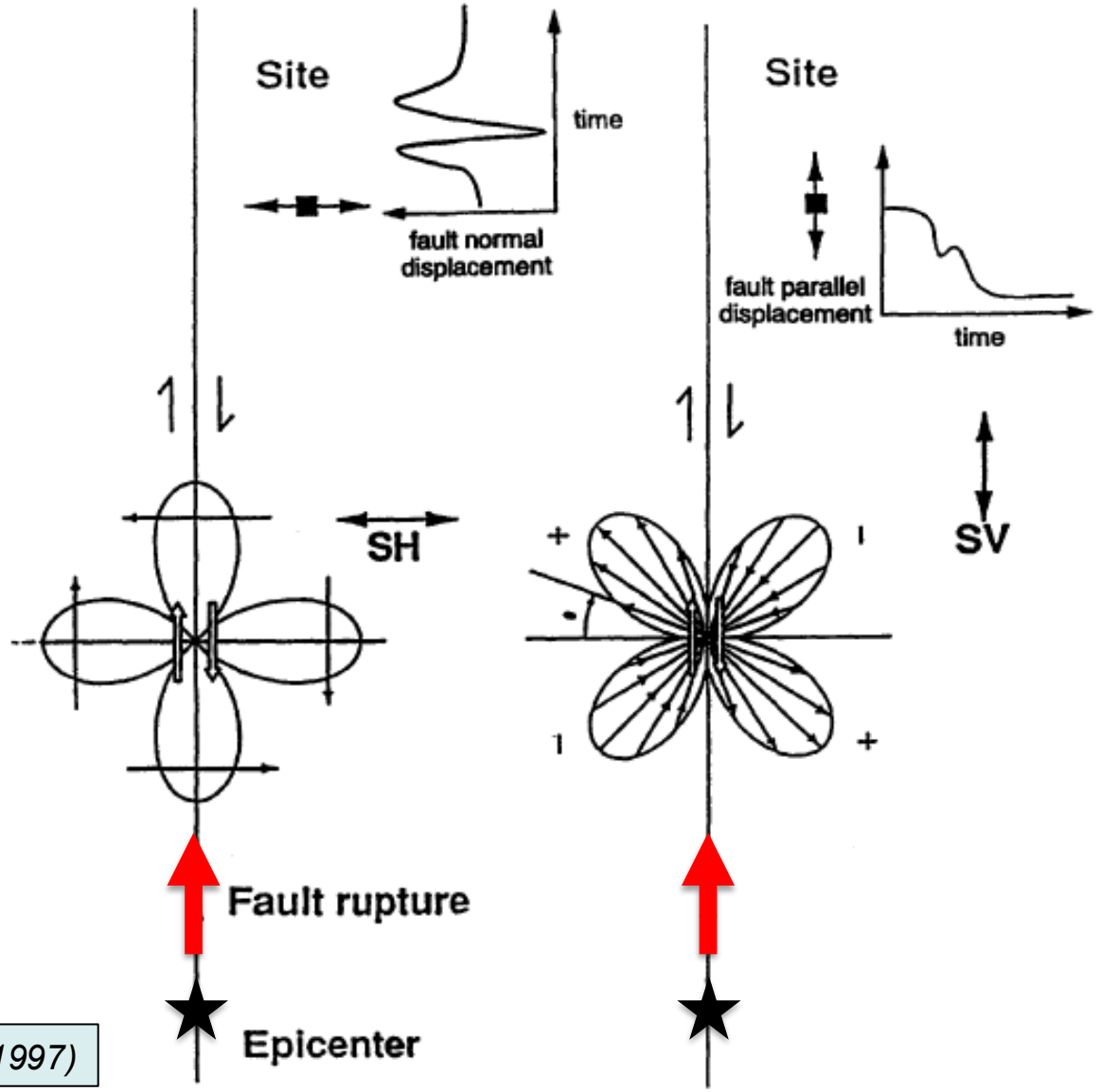

Somerville et al. (1997)

Finite-Fault Rupture Effects

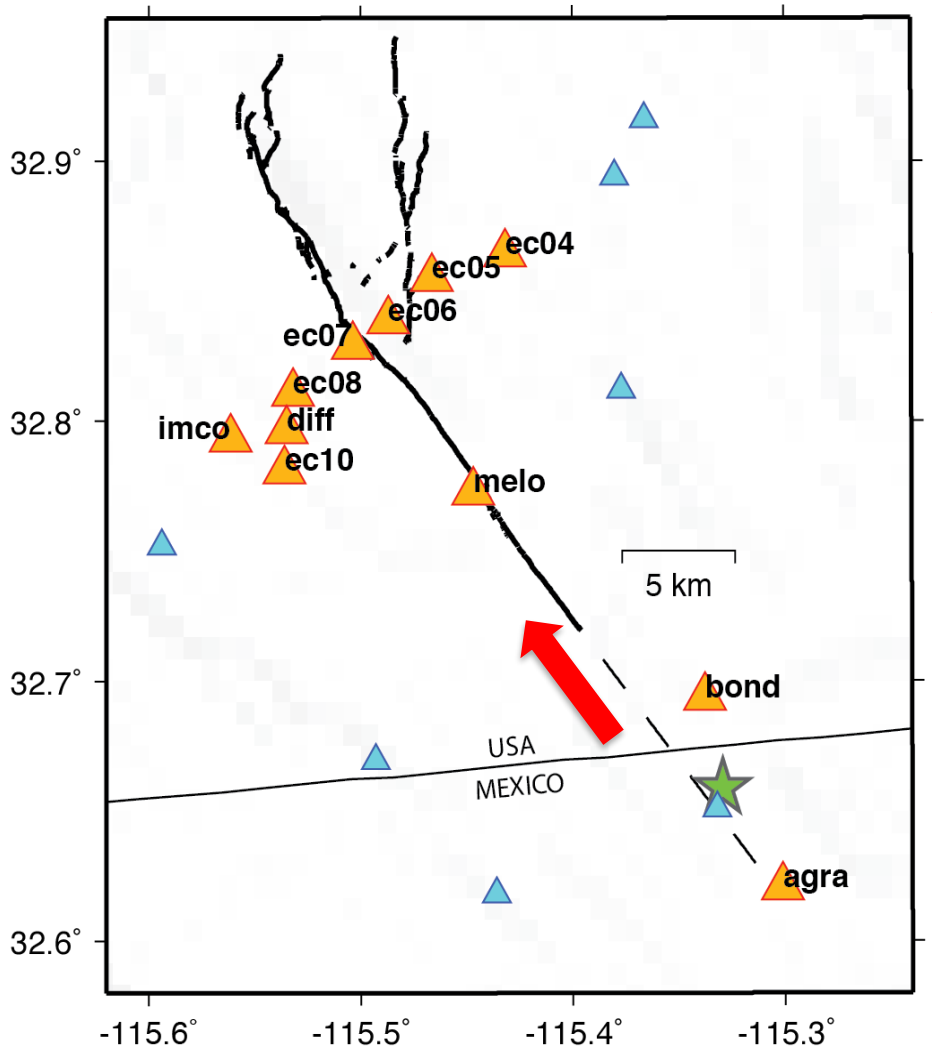

1979 M6.5 Imperial Valley Earthquake

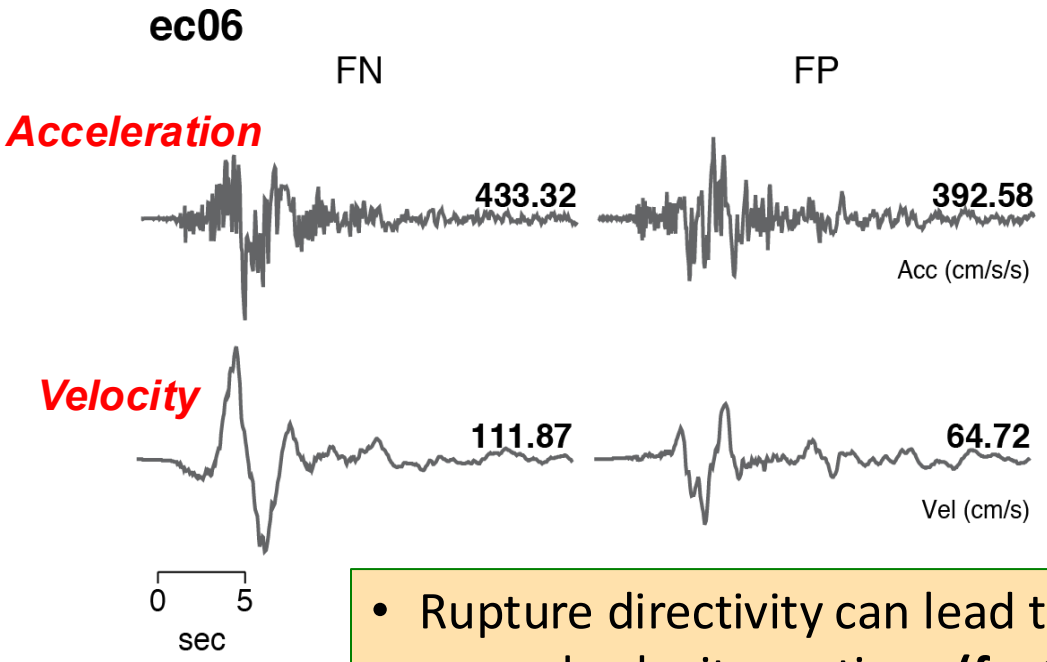

- Rupture directivity can lead to pulse-like ground velocity motions **(f < 1 Hz)**
- Strong polarization onto **Fault Normal** component
- **Higher frequencies (f > 1 Hz)** don't show radiation pattern effects

Archuleta, 1982; Graves and Pitarka (2016)

USGS science for a changing world

Finite-Fault Rupture Effects

Frequency Dependence of Radiation Pattern

- Compute ratio of Fourier amplitude spectra for Fault Normal and Fault Parallel components at 11 near-fault sites (gray lines)
- Average of 11 sites shown in red
- **Fault Normal** larger than **Fault Parallel** component for **f < 1 Hz**
- Average ratio centered around unity for **f > 1 Hz**

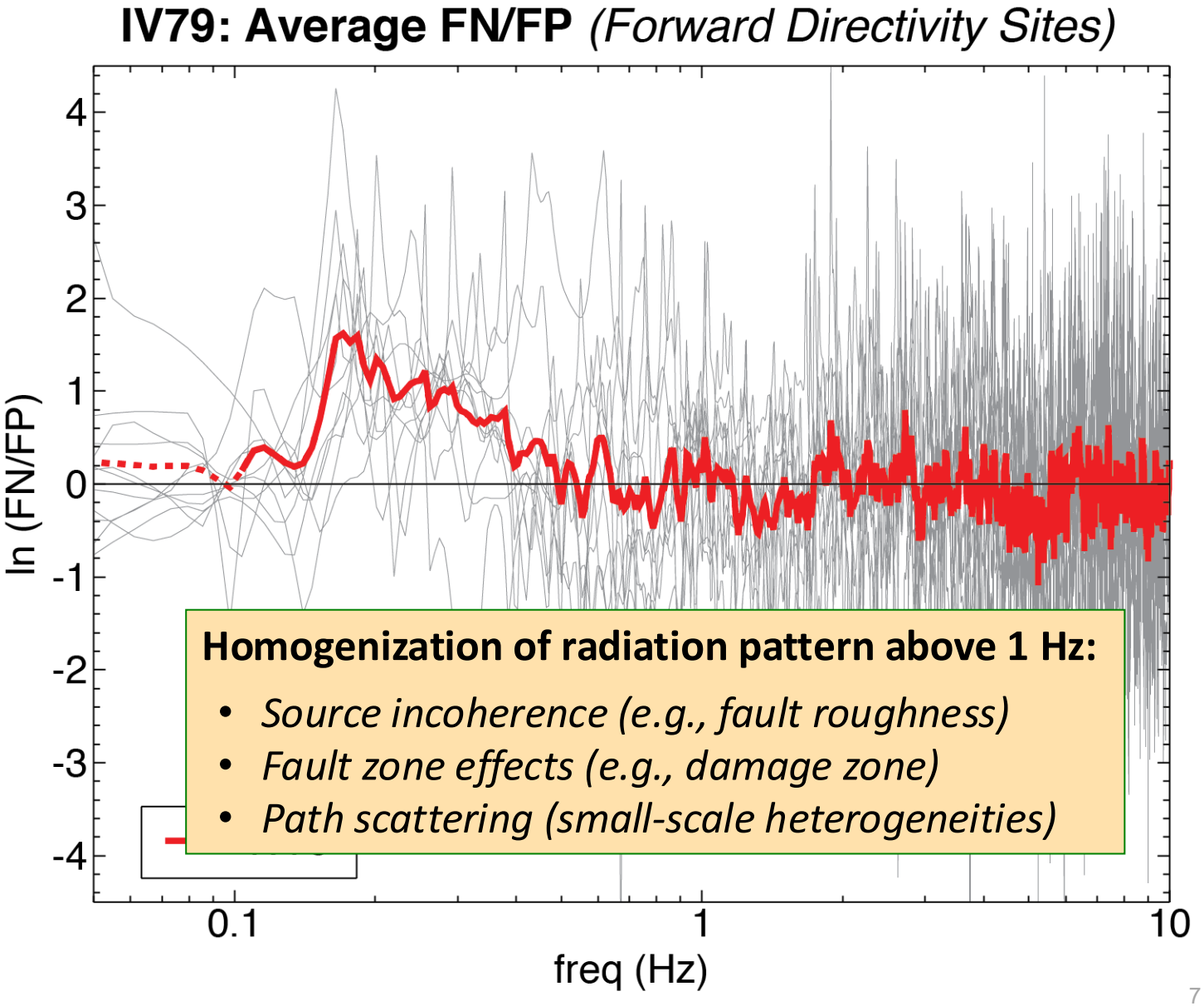

Graves and Pitarka (2016)

USGS science for a changing world

Hybrid Broadband Simulation Method

Hartzell et al. (1999)
Frankel (2009)
Graves and Pitarka (2010)

Low Frequency (f < 1 Hz)

- Complete finite-fault dynamic or kinematic rupture description (spatial and temporal evolution of rupture)
- Full theoretical anelastic wave propagation within 3D velocity structure

➔ ***Deterministic***

High Frequency (f > 1 Hz)

- Simplified finite-fault rupture (generalized rupture time and slip heterogeneity)
- Source radiation has ***stochastic phase*** and average radiation pattern
- Simplified Green's functions (travel time, geometric spreading, attenuation and impedance effects)
- Non-linear V_{s30}-based site amplification factors

➔ ***Stochastic***

** Both approaches utilize deterministic and stochastic features so above classification is not strictly correct.*

USGS science for a changing world

High Frequency (Stochastic) Simulation

Hanks and McGuire (1981)
Boore (1983)

Represent as Fourier transform of ground acceleration waveform $a_j(t)$:

$$\mathbb{F}\{a_j(t)\} = \Sigma_{i=1,N}\, G_{ij}(f)\, S_i(f)\, W_i^*(f)$$

$G_{ij}(f)$: Green's function (path term; e.g., $1/R^x$)

$S_i(f)$: Subfault source amplitude spectrum ("omega-squared" Brune, 1970)

$W_i^*(f)$: Complex spectrum of windowed time series having ***random phase***,
➔ this is the ***stochastic*** part of the ***stochastic*** simulation

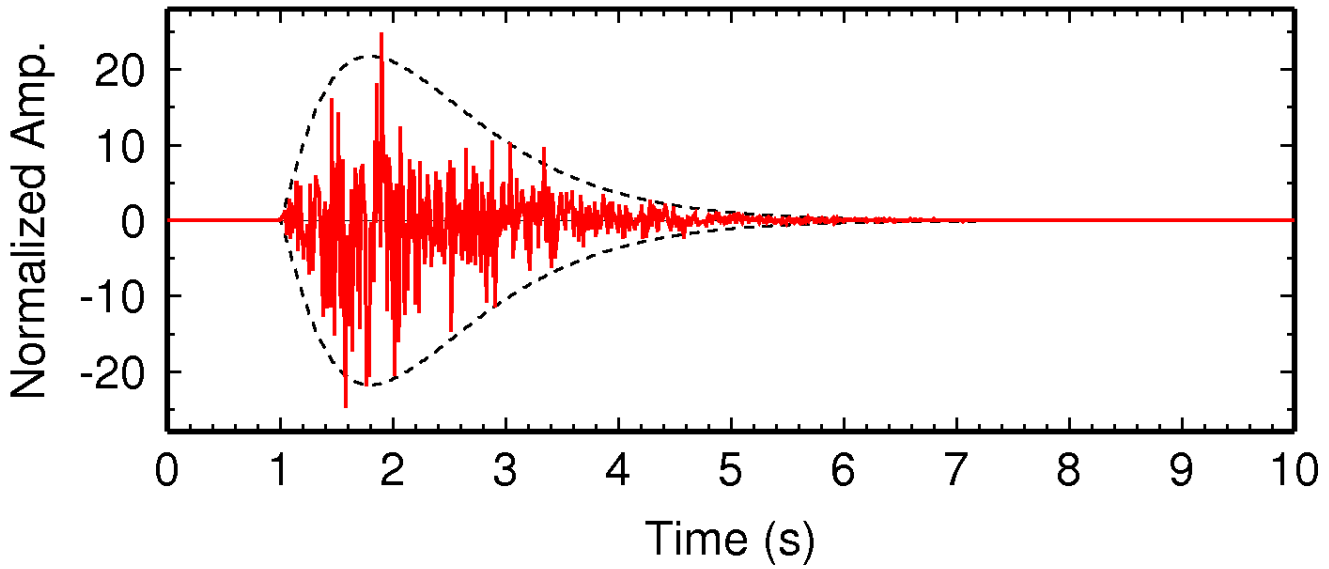

Stochastic Simulation

What does the Stochastic Phasing of $W_i^*(f)$ Represent?

- The stochastic approach (Hanks and McGuire, 1981; Boore, 1983), was designed to match statistical properties of observed **high frequency** ground motions using **a simple, far-field model** of the radiated amplitude spectra.
- There is **no explicit slip-rate function** in the stochastic approach. The **random phasing** within $W_i^*(f)$ represents **unmodeled details** of the rupture process and scattering effects along the propagation path.

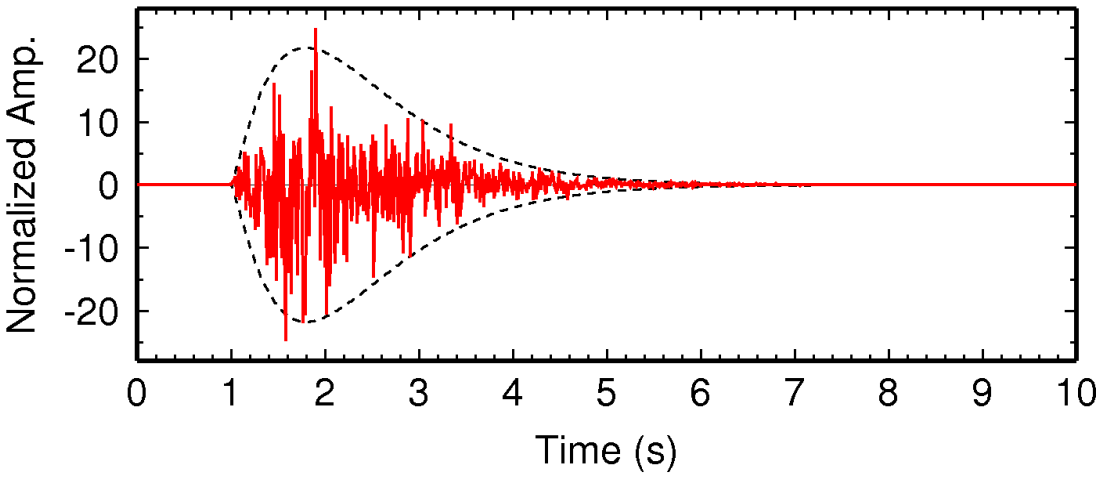

Hybrid Broadband Simulation Method

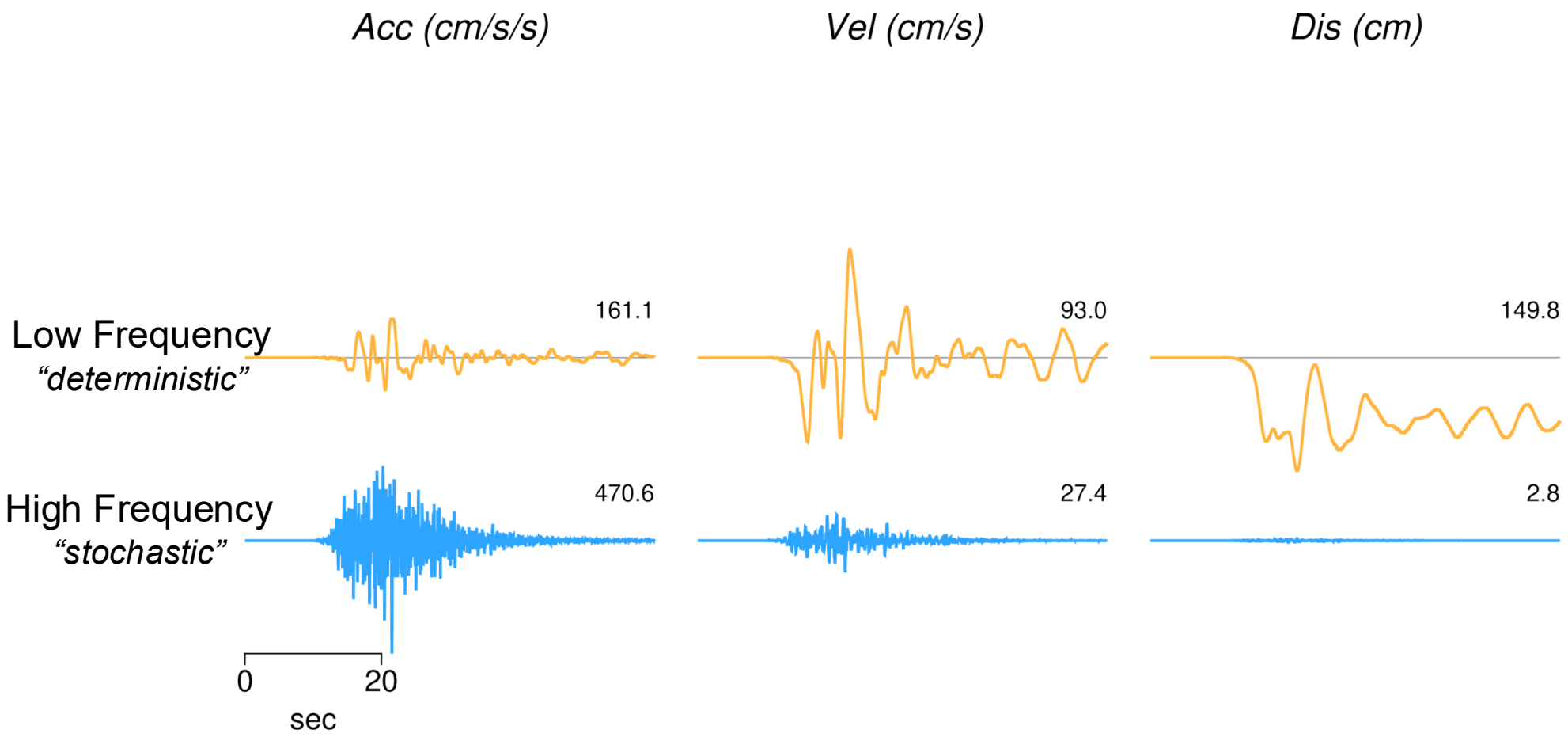

Hybrid Broadband Simulation Method

Match Filtering

Filter and sum to combine separate low- and high-frequency responses into full broadband time series.

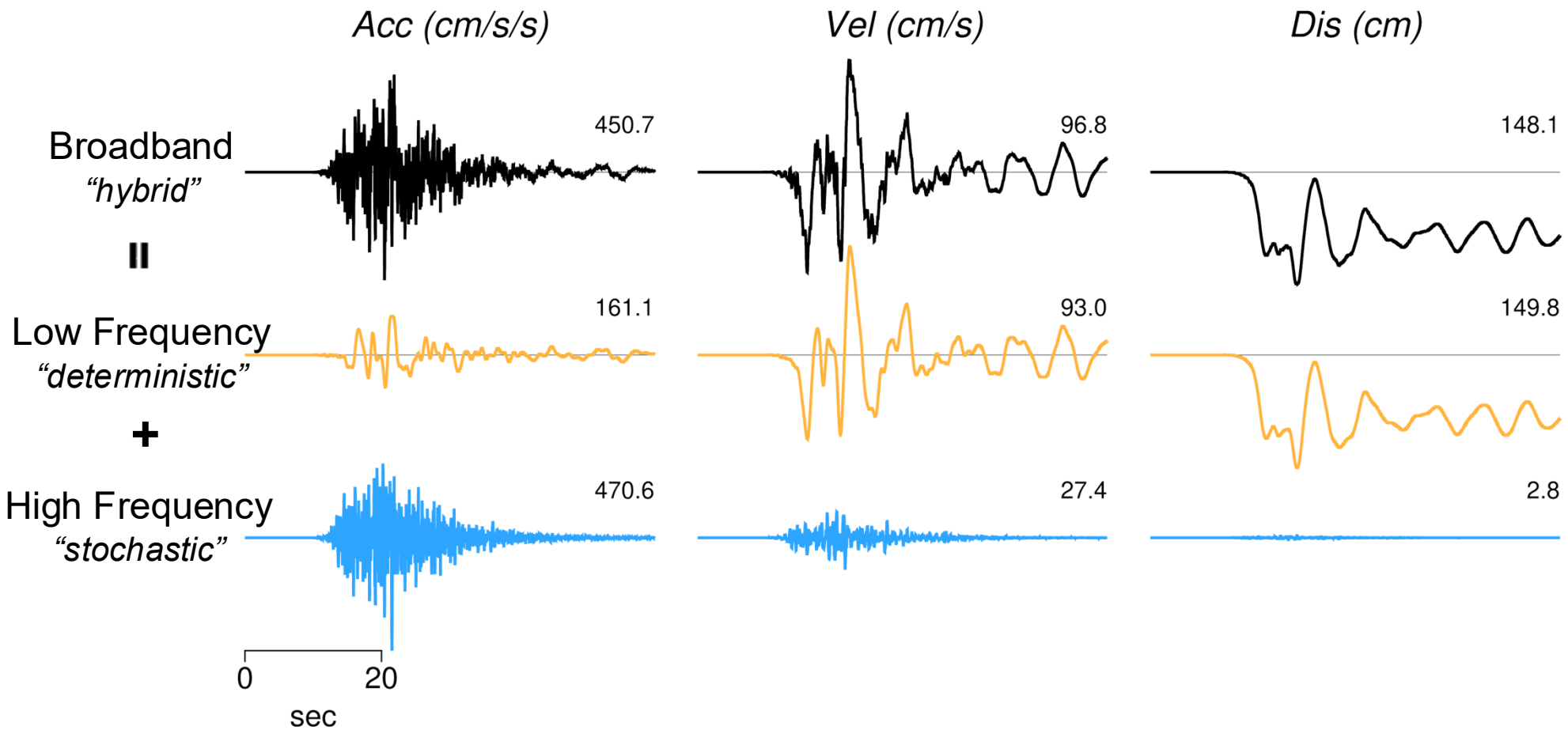

Hybrid Broadband Simulation Method

Match Filtering

Filter and sum to combine separate low- and high-frequency responses into full broadband time series.

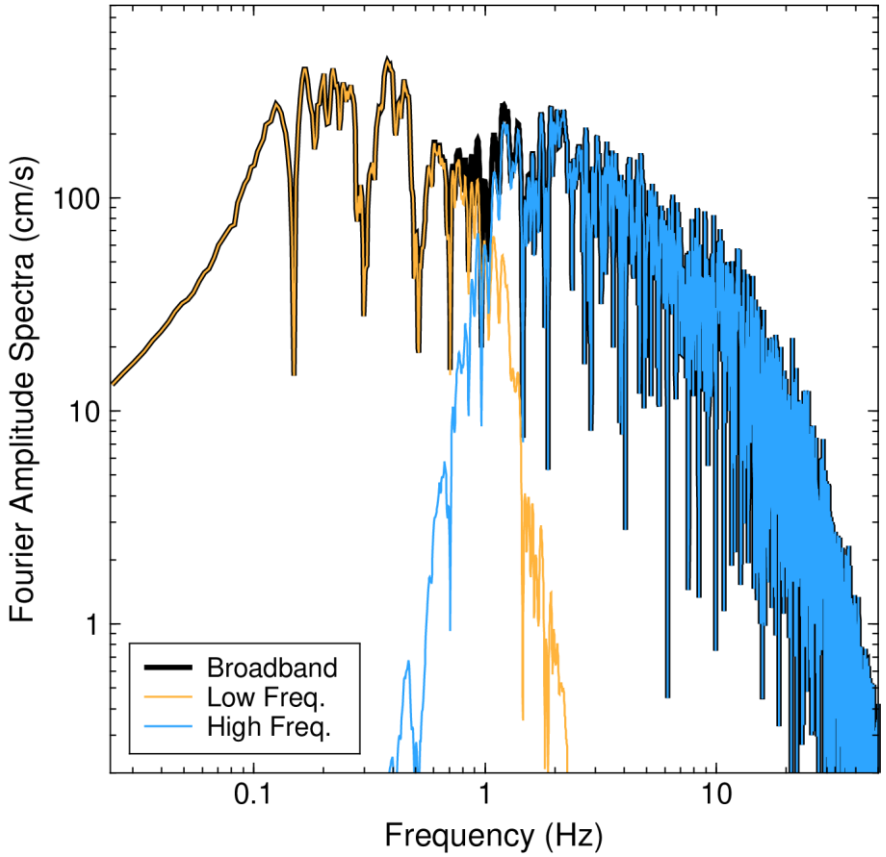

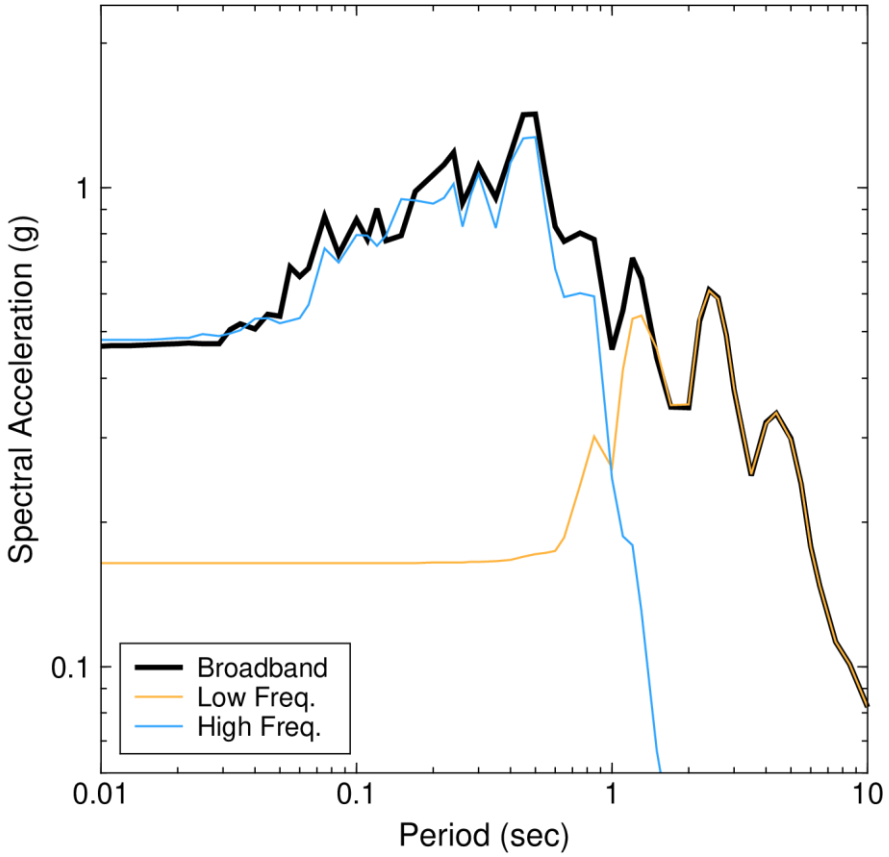

Next Steps

- Continue analysis and verification of low-frequency results
- Define grid of sites where broadband motions will be computed
  - *1-2 km spacing (doesn't need to be uniform)*
  - *Other sites of interest to be included (e.g., seismic stations, Kate's house, …)*
  - *Likely on the order of 100,000 sites*
  - *Provide input for ShakeMap generation and other downstream analyses*
  - *All broadband waveforms to be archived and made accessible for download*
- High-frequency computation currently implemented (and tested) on Frontera @ TACC – exploring other HPC options
- Estimate of 1-2 days to obtain full set of broadband results once "go" button is pushed

Thank You

References

Aagaard, B. T. (2018). Earth Science Research Needs for Improving Earthquake Scenarios, Plenary Presentation, 2018 SCEC Annual Meeting, Palm Springs, CA.

Archuleta, R. J. (1982), Analysis of near-source static and dynamic measurements from the 1979 Imperial Valley earthquake, *Bull. Seism. Soc. Am.*, **72**(6), 1927–1956.

Ben-Zion, Y., F. L. Vernon, Y. Ozakin, D. Zigone, Z. E. Ross, H. Meng, M. White, J. Reyes, D. Hollis and M. Barklage (2015). Basic data features and results from a spatially dense seismic array on the San Jacinto fault zone, *J. Geophys. Int.*, **202**, doi: 10.1093/gji/ggv142.

Boore, D. M. (1983), Stochastic simulation of high-frequency ground motions based on seismological models of the radiated spectra, *Bull. Seism. Soc. Am.*, **73**(6), 1865–1894.

Bouchon, M., Karabulut, H., Bouin, M.-P., Schmittbuhl, J., Vallee, M., Archuleta, R., Das, S., Renard, F., and Mrasan, D. (2010) Faulting characteristics of supershear earthquakes, *Tectonophysics*, **493**, 244–253, doi:10.1016/j.tecto.2010.06.011.

Brune, J. N. (1970). Tectonic stress and spectra of seismic shear waves from earthquakes, *J. Geophys. Res.*, **75**, 4997–5009.

Cochran, E. S., Y.-G. Li, P. M. Shearer, S. Barbot, Y. Fialko, and J. E. Vidale (2009), Seismic and geodetic evidence for extensive, long-lived fault damage zones, *Geology*, **37**(4), 315–318, doi:10.1130/G25306A.1.

Dunham, E. M. and R. J. Archuleta (2004), Evidence for a Supershear Transient during the 2002 Denali Fault Earthquake, *Bull. Seism. Soc. Am.*, **94**(6B), S256–S268.

Ellsworth, W. L., M. Celebi, J. R. Evans, E. G. Jensen, R. Kayen, M. C. Metz, D. J. Nyman, J.W. Roddick, P. Spudich, and C. D. Stephens (2004), Near-Field Ground Motion of the 2002 Denali Fault, Alaska, Earthquake Recorded at Pump Station 10, *EQ Spectra*, **20**(3), 597–615.

References (cont.)

Frankel, A., and R. W. Clayton (1986), Finite Difference Simulations of Seismic Scattering ' Implications for the Propagation of Short-Period Seismic Waves in the Crust and Models of Crustal Heterogeneity, *J. Geophys. Res.*, **91**, 6465–6489.

Frankel, A. (2009). A constant stress-drop model for producing broadband synthetic seismograms: Comparison with the next generation attenuation relations, Bull. Seismol. Soc. Am. 99, no. 2A, 664–680, doi: 10.1785/0120080079.

Graves, R. W., and A. Pitarka (2010). Broadband ground-motion simulation using a hybrid approach, Bull. Seismol. Soc. Am. 100, no. 5A, 2095–2123, doi: 10.1785/0120100057.

Graves, R. W., and A. Pitarka (2016), Kinematic Ground Motion Simulations on Rough Faults Including Effects of 3D Stochastic Velocity Perturbations, *Bull. Seism. Soc. Am.*, **106**(5), doi: 10.1785/0120160088.

Hanks, T. C., and R. K. McGuire (1981). The character of high-frequency strong ground motion, *Bull. Seism. Soc. Am.*, **71**, 2071-2095.

Hanks, T. C. and Bakun, W. H. (2014) M-log A models and other curiosities, *Bull. Seism. Soc. Am.*, **104**(5), 2604–2610, doi:10.1785/0120130163.

Hartzell, S., S. Harmsen, A. Frankel, and S. Larsen (1999). Calculation of broadband time histories of ground motion: comparison of methods and validation using strong-ground motion from the 1994 Northridge earthquake, *Bull. Seism. Soc. Am.*, **89**, 1484–1504.

Hartzell, S., S. Harmsen, and A. Frankel (2010), Effects of 3D Random Correlated Velocity Perturbations on Predicted Ground Motions, *Bull. Seism. Soc. Am.*, **100**(4), 1415–1426, doi:10.1785/0120090060.

Kagawa, T., K. Irikura, and P. Somerville (2004). Differences in ground motion and fault rupture process between surface and buried rupture earthquakes, *Earth Planets Space,* **56**, 3–14.

References (cont.)

Leonard, M. (2010) Earthquake fault scaling: Self-consistent relating of rupture length, width, average displacement, and moment release, *Bull. Seism. Soc. Am.*, **100**(5A), 1871–1988, doi:10.1785/0120090189.

Mai, P. M., and G. C. Beroza (2002). A spatial random field model to characterize complexity in earthquake slip, *J. Geophys. Res,.* **107**(B11), doi 10.1029/2001JB000588.

Milliner, C. W. D., J. F. Dolan, J. Hollingsworth, S. Leprince, F. Ayoub, and C. G. Sammis (2015), Quantifying near-field and off-fault deformation patterns of the 1992 Mw 7.3 Landers earthquake, *Geochem. Geophys. Geosyst.*, **16**, 1577–1598, doi:10.1002/2014GC005693.

Mordret , A., P. Roux, P. Bou ´ e and Y. Ben-Zion (2019), Shallow three-dimensional structure of the San Jacinto fault zone revealed from ambient noise imaging with a dense seismic array, *Geophys. J. Int.*, **216**, 896–905 doi: 10.1093/gji/ggy464.

Nakata, N. and G. C. Beroza (2015), Stochastic characterization of mesoscale seismic velocity heterogeneity in Long Beach, California, *Geophys. J. Int.*, **203**, 2049–2054 doi: 10.1093/gji/ggv421.

Power, W. L., and T. E. Tullis (1991), Euclidean and fractal models for the description of rock surface roughness, *J. Geophys. Res.*, **96**(B1), 415, doi:10.1029/90JB02107.

Rockwell, T. K., and Y. Ben-Zion (2007). High localization of primary slip zones in large earthquakes from paleoseismic trenches: Observations and implications for earthquake physics, *J. Geophys. Res.*, **112**, doi:10.1029/2006JB004764.

Roten, D., K. B. Olsen, S. M. Day, Y. Cui, and D. Fäh (2014), Expected seismic shaking in Los Angeles reduced by San Andreas fault zone plasticity, *Geophys. Res. Lett.*, **41**, 2769–2777, doi:10.1002/2014GL059411.

Seyhan, E., Jonathan P. Stewart, and R. W. Graves (2013), Calibration of a Semi-Stochastic Procedure for Simulating High-Frequency Ground Motions, *EQ Spectra*, **29**(4), 1495–1519.

References (cont.)

Shi, Z., and S. M. Day (2013), Rupture dynamics and ground motion from 3-D rough-fault simulations, *J. Geophys. Res.*, **118**(3), 1122–1141, doi:10.1002/jgrb.50094.

Somerville, P. G., N. F. Smith, R. W. Graves, and N. A. Abrahamson (1997), Modification of Empirical Strong Ground Motion Attenuation Relations to Include the Amplitude and Duration Effects of Rupture Directivity, *Seism. Res. Lett.*, **68**(1), 199–222, doi:10.1785/gssrl.68.1.199.

Somerville, P., K. Irikura, R. Graves, S. Sawada, D. J. Wald, N. Abrahmason, Y. Iwasaki, T. Kagawa, N. Smith, and A. Kowada (1999). Characterizing crustal earthquake slip models for the prediction of strong ground motion, *Seism. Res. Lett.* **70**(1), 59–80.

Thingbaijam, K. K. S., Mai, P. M., and Gosa, K. (2017) New Empirical earthquake source-scaling laws, *Bull. Seis. Soc. Am.*, **107**(5), 2225-2246, doi:10.1785/0120170017.

Trugman, D. T., and E. M. Dunham (2014), A 2D pseudodynamic rupture model generator for earthquakes on geometrically complex faults, *Bull. Seism. Soc. Am.*, **104**(1), 95–112, doi:10.1785/0120130138.

Yamada, M., A. H. Olsen, and T. H. Heaton (2009), Statistical features of short-period and long-period near-source ground motions, *Bull. Seism. Soc. Am.*, **99**(6), 3264–3274, doi:10.1785/0120090067.